MICROSTRUCTURAL ANALYSIS OF ROCK SANDING PRODUCTION USING FINITE ELEMENT METHOD WITH INTERFACE ELEMENTS.

D. Garolera, I. Carol, C. López

Departament d'Enginyeria del Terreny i Cartogràfica,
ETSECCPB, Universitat Politècnica de Catalunya, 08034 Barcelona

Abstract. Rock sanding in oil wells is an erosion process in which grains are disaggregated due to a combination of stress and fluid flow. This process is studied using the finite element method with interface elements and explicit representation of the material microstructure. A cross-section of a small-diameter side perforation of the main well is considered. Within a circular region around the hole, the individual rock grains are discretized, while the space between the ring perimeter and the square domain limits is filled with standard triangular elements. The space within each grain is discretized using elastic finite elements, while the intergranular contact is represented with zero-thickness interface elements equipped with a fracture-based constitutive law. The analysis starts from the initial stress state before the perforation is made. The fluid pressure is progressively decreased inside the hole causing intergranular cracks to develop and coalesce. After the analysis it has been possible to conclude that: a) the evolution of fracture around the hole can be represented realistically by this model, b) the size effect of the perforation diameter may be capturated thanks to the micromechanical approach.

Resumen. La producción de arena (*rock sanding*), en perforaciones petrolíferas, es un proceso erosivo causado por una combinación de tensiones y fuerzas de arrastre. Este proceso es estudiado mediante el método de los elementos finitos con elementos de interfase y la representación explícita de la microestructura del material. Para ello, se modela la sección transversal de una perforación lateral de pequeño diámetro. Por un lado, se discretizan los granos individuales de roca dentro de un anillo circular alrededor del agujero, mientras que el resto se llena con elementos triangulares estándar. El espacio dentro de cada grano se discretiza con elementos finitos de comportamiento elástico, mientras que los contactos intergranulares se representan con elementos junta sin espesor con ley constitutiva frágil. El análisis comienza imponiendo el estado de tensiones iniciales previo a la perforación. Luego, la presión del fluido en el interior de la perforación se disminuye progresivamente, lo cual da lugar a la generación y propagación de la fisuración. Las conclusiones más interesantes han sido: a) la representación realista de la evolución de la fisuración, b) el efecto de tamaño del diámetro de la perforación puede ser detectado gracias al enfoque micromecánico.

1 INTRODUCTION

Sand production is a disintegration phenomenon which takes place in weak rocks such as unconsolidated sandstones. This process is governed by several factors, among which the stress level and the drawdown pressure appear to be the most important. The former controls the fracture of the media and the latter is the responsible for transport of the disaggregated material [1].

The study of sand production in oilfield wells has been an important investigation subject during last decades, since new drilling techniques, such as perforating guns, have been in use. The perforating gun technique consists of introducing a tube with lateral orifices (Fig. 1a) with an explosive charge inside. This device is placed into the borehole and the explosive is detonated, thus generating a large number of lateral perforations (Fig. 1b). The characteristics of these lateral perforations are function of size and distribution of tool orifices. For example a common perforation diameter is around 2cm.

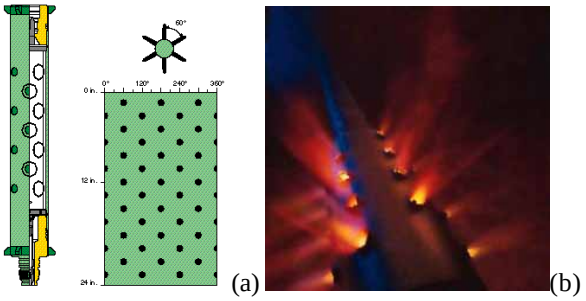


Fig. 1. Perforating gun [2].

Due to the excavation technique (explosives) and to the small diameters involved, side perforations do not allow casing and therefore become potential sites for rock sanding production.

Several authors have studied the problem of rock sanding in small perforations. In this introduction we highlight two types of studies: experimental investigations, and numerical modelling.

1.1 Experimental studies

Perhaps the most interesting experimental tests on rock sanding have been performed with cylindrical samples. This kind of tests, which have been carried out by different authors [1]-[3-5], consists of a cylinder with an axial perforation, which is introduced into a modified triaxial cell. In this cell, fluid flow along the central hole and in the radial direction may be prescribed in addition to the traditional radial and axial stresses.

The results of these studies have allowed to conclude that the variation of effective stress between the grains is the main responsible for the integranular fracture, while the fluid flow works like a transport agent [1].

1.2 Numerical studies

Existing numerical studies of rock sanding may be classified into two major types: the continuum (macroscopic) approach and the discrete (micromechanical) approach.

In the continuum approach, the problem is studied from a macroscopic viewpoint using the finite element method (FEM), mainly through wellbore stability analysis. This methodology only describes the initial sanding conditions. *Vardoulakis et al*.[7], for instance, have proposed a combination of a damage formulation (bifurcation theory) and solid transport equations. This technique allows predicting the onset of rock sanding and its evolution; however it needs parameters which in general are difficult to obtain.

The discrete approach is based on the discretization of the rock grains. Until now, this type of modelling had been mainly applied using the distinct element method (DEM), for instance see *Jensen et al*. [8]. This methods seems good because is able to explain both the rock sanding initiation and follow then each particle, thanks to the explicit nature of the formulation. However, the major constraint comes from the considerable calculation times needed to solve each iteration.

2 MICROSTRUCTURAL MODELLING

2.1 Microstructure

In this study, the grain geometry has been generated by automatic algorithms based on Delaunay-Voronoi standard procedures that create a random distribution of grains, which was initially developed for mesh generation in trabecular bone simulation [9]. The grains are discretized using standard triangular finite elements with linear elastic behaviour. An example of this type of mesh is given in Fig.2b, which can be compared to a real sample of sandstone from an oil well (Fig. 2a)

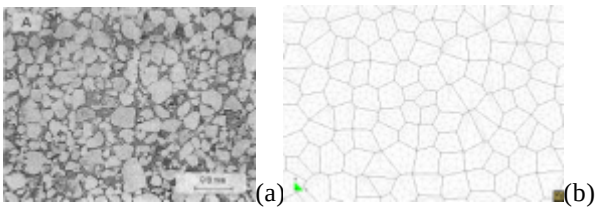


Fig. 2. Comparison between real (a) and numerical (b) distribution of the grains. (Microphotography courtesy from Schlumberger Cambridge Research)

The contacts between grains are modelled by means of zero-thickness interface elements equipped with a non-linear constitutive law capable of representing the fracture process. The law is formulated in terms of normal and shear stress tractions and the corresponding relative displacements. The evolution is controlled by the fracture energy spent in the developing crack, which drives the evolution of σ (tensile strength), c (cohesion) and $\tan(\phi)$ (friction angle), all them parameters of the hyperbolic loading surface. Details about this model may be found in [10], [11] and [12].

2.2 Cross-section discretization

A 2-D cross-section of a perforation perpendicular to the main well (Fig. 3) has been considered for this study.

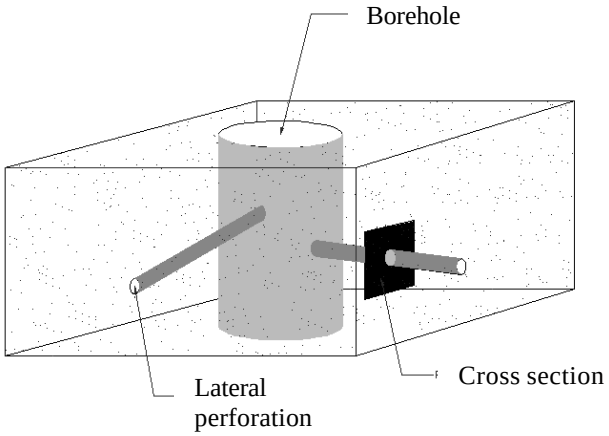


Fig. 3. Scheme of the real problem. In black, cross-section considered for the analysis.

For economy reasons, the discretization of the rock medium has been separated in two parts:

1. A circular ring around the hole where the grains are explicitly represented by a random distribution of triangular finite elements with linear elastic behaviour, separated by interface elements (Fig. 4a), in the way described in § 2.1.
2. A continuum mesh is generated around the previous zone in order to fill up the space between the outer boundary of the ring and the external limits of the square domain (Fig. 4b). This part is generated with a standard mesh generator, in this case GID.

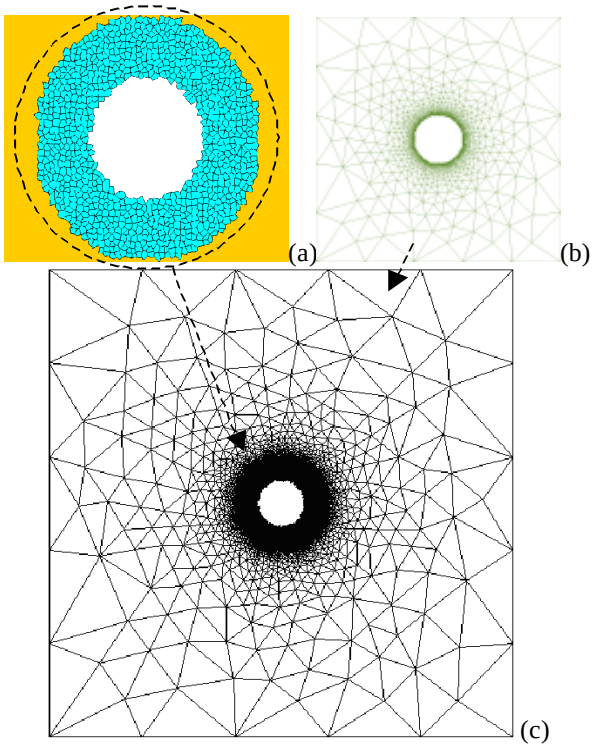


Fig. 4. Discretization process: (a) initial discrete mesh, (b) continuum mesh from GID discretization, and (c) full mesh.

The elastic parameter values used for the continuum grains are given in Table 1. The parameters used for the interface constitutive model, corresponding to a weak sandstone, are also given in the same table. However it has to be noted that for this exploratory study these values have been estimated from the limited data available. In more advanced studies aiming at quantification, specific tests will be necessary for parameter determination.

Table 1. Constitutive parameters used in calculations.

Continuum medium		
Specific weight (ρ)	0.0023	(Kgf/cm^3)
Young modulus (E)	25,000	(Kgf/cm^2)
Poisson modulus (ν)	0.27	(Kgf/cm^2)
Discrete medium		
Normal stiffness (K_n)	5,000,000	(Kgf/cm^2)
Tangent stiffness (K_t)	5,000,000	(Kgf/cm^2)
Friction angle (φ)	24	(^{o})
Normal tensile strength (χ_o)	0.1	(Kgf/cm^2)
Cohesion (C)	0.40	(Kgf/cm^2)
Fracture energy (mode I)	0.00001	(Kgf*cm)
Fracture energy (mode IIa)	0.0001	(Kgf*cm)

2.3 General settings

Concerning loads and general aspects of the calculations, the following is noted:

Hypotheses

1. For simplicity, this first series of calculations are made in total stresses. The pressure decrease in the perforation is represented as a decrement of the normal stress applied on the hole surface.
2. The grain size used in this analysis is 1 mm, which is 2-5 times greater than the real one according the available images. Nevertheless, it is considered that this is enough to capture essential qualitative features of the model proposed.
3. The calculations are all made assuming small deformations, which should be enough at least in the firsts steps of sand production.
4. Due to the limited discretization of the microstructural geometry, with a limited number of grains around the hole, the sanding process can be followed only while cracks do not get too deep into the rock. This, however, will not represent a real limitation in this preliminary study concentrated in initial cracking.
5. The direct effects of axial flow have not been considered explicitly due to the nature of the approach. In this context, it is considered that once isolated by cracks, the grains are taken away by the fluid.

Methodology

The simulation process has been divided in different parts (see Fig. 5):

1. Generation of the initial stress state. Two cases have been distinguished: first, hydrostatic stress state with initial stress ($\sigma_y = \sigma_x = 150$ kgf/cm^2, corresponding to a rock cover of about 625m). Second, a non-hydrostatic initial stress state with K_0=2, ($\sigma_h = 150$ kgf/cm^2, $\sigma_v = 75$ kgf/cm^2).
2. Simulation of the pressure decrease inside the hole due to the drawdown process. During this stage, some interfaces start cracking. A grain removing criterion is adopted to simulate the disappearance of grains due to the erosion process. In the non-hydrostatic case, between the compression step and the unloading process, the excavation procedure has been simulated using the corresponding feature of the computer code (the elements are removed, and the equivalent nodal forces are applied to the remaining part of the mesh). The excavation forces have been accompanied by simultaneous application of the internal fluid pressure, assumed initially in this case 50 kgf/cm^2.

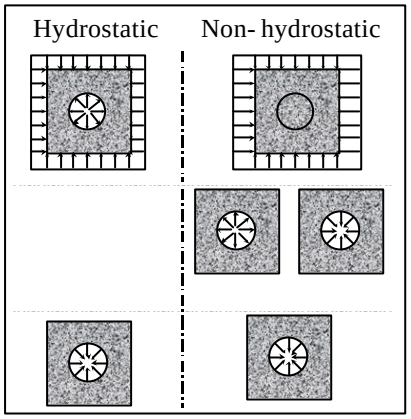


Fig. 5. Scheme of calculation steps. Left column, hydrostatic initial stress. Right column, non-hydrostatic initial stress.

Sanding criteria

A double criterion has been imposed to determine when a grain must be removed. First, a criterion based on fracture energy spent at a point of the grain perimeter (W^{cr}) is used to decide when the interface is broken according to Eqns. (1). Second, a methodology is established to describe which grain or grains have to be removed. This second algorithm has not been implemented yet as an automatic process due to time limitations.

$$\left.\begin{array}{l} \text{mode I}: \text{coef} = \dfrac{W^{cr}}{G_f^{I}} \\ \text{mode IIa}: \text{coef} = \dfrac{W^{cr}}{G_f^{IIa}} \end{array}\right\} \text{break if coef} \geq 0.8 \qquad (1)$$

3 RESULTS

In this paper, three examples are provided to demonstrate the qualitative good performance of this methodology:

1. Perforation diameter 2cm with hydrostatic state of initial stress.
2. Size effect study. A comparative analysis using different perforation diameters.
3. Perforation diameter 2cm with non-hydrostatic initial stress state ($K_0 = 2$).

3.1 Hydrostatic initial stress

The long-term objective of this study will be to obtain the relation between the amount of eroded sand and the pressure decrease inside the hole. For this purpose a mesh like (Fig. 4c) has been generated with the geometric characteristics given in Table 2.

Table 2. Dimensions of discretization.

Mesh characteristics		
Perforation diameter	2	(cm)
Grain size	1	(mm)
Number of nodes	20,036	
Number of elements	26,896	
Number of interface elements	5,474	

Interesting results in terms of qualitative behavior are obtained in this case. The evolution of intergranular fracture with progressive decrease of downhole pressure is represented in the sequence of Fig. 6a, 6b, and 6c., for pressures down from 150 to about 46 Kg/cm^2.

After writing this paper, the calculations continue to reduce the downhole pressure even further and eventually to zero. In the results obtained so far, no grains have become totally detached yet from the hole wall. However in the latest stage (Fig. 6c) a few interfaces have already overcome the limit (1). These are represented in more detail Fig. 7, where it is possible to observe some groups of grains approaching the sanding condition.

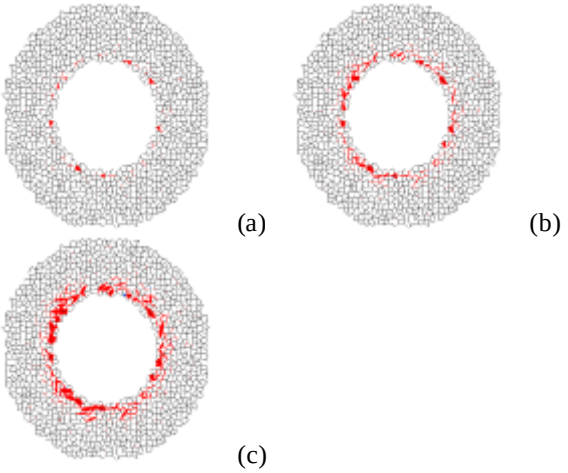


Fig. 6. Cracking evolution where each picture represents a different load increment. The thickness of the lines symbolizes the fracture energy spent in each interface.

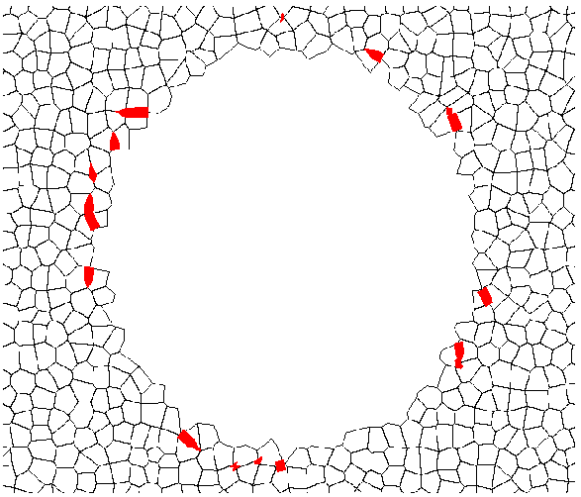


Fig. 7. Fractured interfaces that have reached the open crack criterion (although no grain or group of grains has become completely surrounded by open cracks).

3.2 Size effect study

The objective of this example is to demonstrate that this methodology can capture the size effect of the perforation diameter. For this purpose, two more cases with diameters of 1 and 0.5cm have been considered (Table 3).

Table 3. Dimensions of mesh in size effect modelling.

Mesh characteristics	Small	Medium	Large	
Perforation diameter	0,5	1	2	(cm)
Grain size	1	1	1	(mm)
Number of nodes	10,773	13,818	20,036	
Number of elements	14,792	18,738	26,896	
Number of interface elements	2,840	3,716	5,474	

The results, depicted in Fig. 8, represent the cracking state for the three cases at the same downhole pressure level of 46.25 kgf/cm^2. It can be observed very clearly that the larger the hole, the more extensive the cracking has developed, which represents a significant size effect.

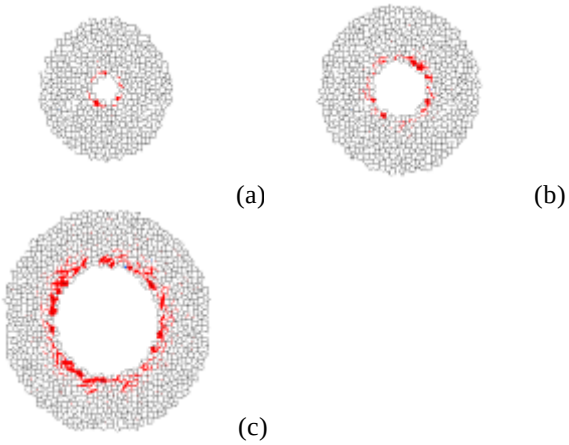


Fig. 8. Fracturation at 46 kgf/cm2 for the different geometries: a) ∅=0.5 cm, b) ∅=1 cm and c) ∅=2 cm.

Another interesting aspect is the downhole pressure level at which the iterative solution process becomes slower and therefore more time consuming. In general terms, this may be linked to the point in the process when micro-fracture becomes widespread, and it also shows how this happens much earlier for the large hole than for the small hole (Table 4).

Table 4. Initiation of micro fracture in size effect study case.

Results	Small	Medium	Large	
Initiation of micro-fracture	80	52.5	42.5	(kgf/cm^2)

3.3 Non-hydrostatic initial stress

A non-hydrostatic initial stress state has been considered, with different values in the x and y directions. In this situation, experiments indicate a dominant tensile cracking on the plane perpendicular to the minimum compression direction, and dominant shear/compression and spalling at 90 degrees from that.

In this case, the remote stresses are first applied on an initial mesh without the hole, and then the hole is "excavated" following the standard procedure implemented in the program, while simultaneously applying the downhole initial pressure. Finally, the downhole pressure has been decreased progressively. As expected, the results obtained are different from previous cases. Fig. 9 depicts a cracking state obtained for K_0=2. As it is clearly shown, these results qualitatively agree with experimental observations.

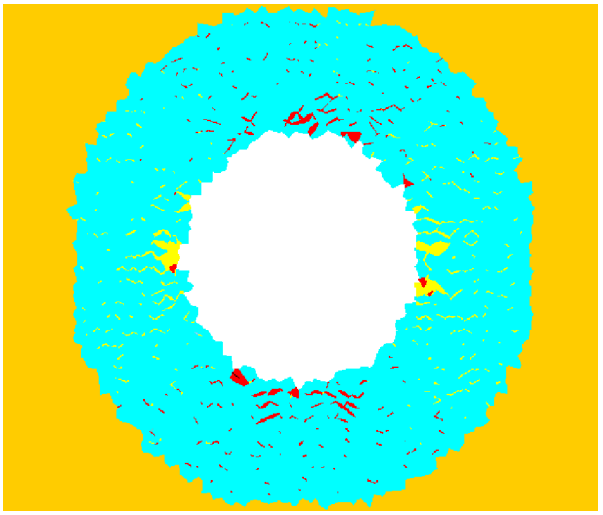


Fig. 9. Fracture at 6 kgf/cm^2.in the non-hydrostatic case. In dark, loaded fractures, in light, unloaded fractures.

4 CONCLUDING REMARKS

This paper describes the initial phases of an on-going study of the rock sanding process in oil wells in weak sandstones, using micromechanical representation of the material around the perforation hole. The methodology employed, finite elements method with fracture-based zero-thickness interface elements, had been previously used successfully in the simulation of the mechanical behaviour of concrete specimens subject to a variety of load scenarios.

Three examples of application have been presented, in which the initial pressure in the hole is reduced progressively. The results exhibit realistic crack patterns in both the cases of hydrostatic and non-hydrostatic state of initial stresses. Also, the size effect

of the hole diameter is captured very clearly, which is a remarkable feature of this approach.

However, this study is only at a preliminary stage, and includes significant simplifications such as that of total stress analysis (no pore pressure/effective pressure decomposition). On-going efforts are directed at continuing the reduction of downhole pressure to reach the point where grains can be effectively eliminated, and to achieving quantitative predictions of sand production. Another priority is to switch to a pore pressure analysis with interface behaviour in terms of effective stress tractions.

5 ACKNOWLEDGEMENTS

The authors wish to thank the collaboration of Schlumberger Cambridge Research, and in particular of Dr. Panos Papanastasiou, for the technical support on the sand production information and valuable comments of various aspects of the study, as well as the help of Olga Roa for the generation of the basic Voronoi mesh for the discretization process. The first author wants to acknowledge the support received from the "Ajut a Grups Consolidats" 2001/SGR/00237 awarded by DURSI (Generalitat de Catalunya) to the Department of Geotechnical Engineering and Geo-Sciences UPC. The second and the third authors wish to acknowledge grants MAT 2000-1007 and BTE2001-2227 from MCYT (Madrid, Spain). Finally, travel support from ETSECCPB-UPC to attend the meeting of the "Grupo Espanol de Fractura" is also greatly appreciated.

6 REFERENCES

[1] Cook, J.M., Bradford, I.D. and Plumb, R.A. "A study of the physical mechanisms of sanding and application to sand production prediction". Presented in *European Petroleum Conference* in London, UK, October 1994. *SPE paper* No. 28852, 1994.

[2] Schlumberger web site: http://www.slb.com /oilfield/Docs/connect/completion/Perforating_Gun _Systems/5hsd.pdf.

[3] Nicholson, E.D., Goldsmith, G. and Cook, J.M. "Direct observation and modeling of sand production processes in weak sandstone". Presented in *SPE/ISRM Eurock '98* in Trondheim, Norway, 8-10 July 1998. *SPE paper* No. 47328, 1998.

[4] Papanastasiou, P., Cook, J. and Durban, D. "Modes of fracture initiation in thick-wall cylinder experiemnts". *Rock Mech. for Industry*, editors Amadei, Kranz, Scott and Smeallie, p. 333-340. Balkema (Rotterdam). ISBN 90-5809-052-3, 1999.

[5] Papanastasiou, P., Nicholson, E.D., Goldsmith, G. and Cook, J. "Sanding prediction: Experimental results and numerical modeling". *Poromechanics*, editores Thimus et al., p 457-462. Balkema (Rotterdam). ISBN 90-5809-003-5, 1999.

[6] Van den Hoek, P.J., Hertogh, G.M.M., Kooijman, A.P., de Bree, Ph., Kenter, C.J. and Papamichos, E. "A new concept of sand production prediction: theory and laboratory experiments". *SPE drill and completion*, Vol. 15 (4), p. 261-273, 2000.

[7] Vardoulakis, I., Stavropoulou, M. and Papanastasiou, P. "Hydromechanical aspects of sand production problem". *Transport in Porous Media*, Vol. 22, p. 225-244, 1996.

[8] Jensen, R.P., Preece, D.S., Cook, B.K. and Williams, J.R. "Modeling sand production with Darcy-Flow coupled with discrete elements". *Comp. Meth. And Adv. In Geomech*, editors Desai et al., p. 819-822. Balkema (Rotterdam). ISBN 90-5809-183-X, 2001.

[9] Roa, O., López, C.M., Maranzana, F., Carol, I. and Contro, R. "On the use of generated geometries for the numerical analysis of trabecular bone specimens". *Computer Methods in Biomechanics and Biomedical Engineering*, Proceedings of the Int. Conf. in Rome (Oct 2001), editor Middlenton, J. 2001.

[10] López, C. M. "Análisis microestructural de la fractura del hormigón utilizando elementos finitos tipo junta. Aplicación a diferentes hormigones.". PhD. Thesis. Escuela Técnica Superior de Ingenieros de Caminos Canales y Puertos. Universitat Politècnica de Catalunya,. 1999. (in Spanish)

[11] Carol, I., Prat, P. and López, C. M. "A normal/shear cracking model. Application to discrete crack analysis" *ASCE J. Engrg. Mech.*, Vol 123(8), p. 765-773, 1997.

[12] Carol, I., López, C. M. and Roa, O. "Micromechanical analysis of quasi-brittle materials using fracture-based interface elements" *Int. J. Num. Methods in Engineering*, Vol 52(1-2), p. 193-215, 2001.

[13] Garolera, D. "Estudio microestructural del rock sanding.". Degree thesis. Escola Tècnica Superior d'Enginyers de Camins Canals y Ports de Barcelona. Universitat Politècnica de Catalunya,. 2003. (in Spanish)